

Phonon spectroscopy near phase transition temperatures in multiferroic BiFeO₃ epitaxial thin films

R. Palai,^{1,*} J. F. Scott,² and R. S. Katiyar¹¹*Department of Physics and Institute for Functional Nanomaterials, University of Puerto Rico, San Juan, Puerto Rico 00931-3343, USA*²*Department of Physics, Cavendish Laboratory, University of Cambridge, Cambridge CB3 0HE, United Kingdom*

(Received 25 September 2009; revised manuscript received 29 December 2009; published 29 January 2010)

We report a Raman-scattering investigation of multiferroic bismuth ferrite (BiFeO₃) epitaxial (*c*-axis-oriented) thin films from -192 to 1000 °C. Phonon anomalies have been observed in three temperature regions: in the γ phase from 930 to 950 °C; at ~ 370 °C, Néel temperature (T_N), and at ~ -123 °C, due to a phase transition of unknown type (magnetic or structural). An attempt has been made to understand the origin of the weak phonon-magnon coupling and the dynamics of the phase sequence. The disappearance of several Raman modes at ~ 820 °C (T_c) is compatible with the known structural phase transition and the *Pbnm* orthoferrite space group assigned by Arnold *et al.* [Phys. Rev. Lett. **102**, 027602 (2009)]. The spectra also revealed a *noncubic* β phase from 820 – 930 °C and the same *noncubic* phase extends through the γ phase between 930 – 950 °C, in agreement with Arnold *et al.* [Phys. Rev. B (to be published)], and an evidence of a cubic δ phase around 1000 °C in thin films that is not stable in powder and bulk. Such a cubic phase has been theoretically predicted by and Gonzalez-Vazquez and Iniguez [Phys. Rev. B **79**, 064102 (2009)]. Micro-Raman scattering and x-ray diffraction showed no structural decomposition in thin films during the thermal cycling from 22 – 1000 °C.

DOI: [10.1103/PhysRevB.81.024115](https://doi.org/10.1103/PhysRevB.81.024115)

PACS number(s): 77.55.-g, 78.30.-j, 77.80.B-, 78.66.Nk

I. INTRODUCTION

Multiferroics are the materials which display a coexistence of at least two of the switchable states: polarization, magnetization, or strain in the same phase.¹ In addition, they may also exhibit a magnetoelectric (ME) effect: magnetization induced by an electric field and electric polarization by means of magnetic field.² The current interest in multiferroics is largely based on engineered epitaxial and heterostructured thin films because their physical properties are as good as bulk and permit technological applications in data storage, magnetic recording, spintronics, quantum electromagnets, and sensors.^{3–5} Devices made up of multiferroic materials can perform more than one task and facilitate device miniaturization. A weak ME effect has been observed in most multiferroics, generally showing a small change in their spontaneous polarization under applied magnetic field.^{2,6,7} However, the complete switching of ferroelectric domains by applied magnetic fields has rarely been observed. Why and under what circumstances a large coupling should exist and how to control the coupling are still open questions. Understanding the physics of the different possible interactions between magnetic and electric order parameters, i.e., giving rise to ME coupling would be very useful.

Magnetism and ferroelectricity are involved with local spin ordering and off-center structural distortions, respectively.⁸ These are quite complementary phenomena that coexist in certain multiferroic materials. Currently, BiFeO₃ (BFO) is one of the most widely studied multiferroics because it is one of only two or three single-phase multiferroics at room temperature, i.e., an antiferromagnetic (AFM) incommensurate phase with cycloidal modulation ($\lambda \approx 60$ nm) below ≈ 370 °C,^{9,10} ferroelectric up to ≈ 820 °C,¹¹ and ferroelastic between 820 – 930 °C.¹² Bulk BFO crystallizes in a rhombohedral ($a=5.58$ Å and

$\alpha=89.5^\circ$) structure at room temperature (RT) with space group $R3c$ (C_{3v}^6) and antiferromagnetism of *G* type.^{10,13} The structure and properties of bulk BFO have been studied extensively^{10,13–15} and although early values of polarization were low ($P_r=6.1$ $\mu\text{C}/\text{cm}^2$) due to sample quality, $P_r=40$ – 100 $\mu\text{C}/\text{cm}^2$ was recently found in bulk by several different groups.^{16,17} The epitaxially grown thin films of BFO on SrTiO₃ (STO) substrates show very high values of P_r (~ 100 $\mu\text{C}/\text{cm}^2$) (Ref. 3) compared to the best known ferroelectrics such as PbZrTiO₃ (~ 70 $\mu\text{C}/\text{cm}^2$) and BaSrTiO₃ (~ 30 $\mu\text{C}/\text{cm}^2$). This makes BFO a potential material for novel device applications.

The motivation for the present study is manifold. The first objective is to test the recent space group determination of the γ phase reported by Arnold *et al.*¹⁸ as being orthorhombic. Their definitive neutron study showed that the γ phase is indeed stable (which in itself had been controversial) and that it has the same orthorhombic *Pbnm* orthoferrite symmetry as does the β phase. A cubic $Pm\bar{3}m$ perovskite structure was definitely ruled out although a body-centered orthorhombic space group was indistinguishable from the primitive *Pbnm*. A main aim of our Raman study is to test the orthorhombic crystal class for the γ phase and see whether we can further distinguish between primitive and body-centered orthorhombic structures.

II. EXPERIMENTAL DETAILS

We investigated 300 nm (001)BFO thin films on STO(100) substrates with ~ 25 -nm-thick SrRuO₃ (SRO) buffer layer by pulsed laser deposition (PLD). A Jovin Yvon T64000 micro-Raman microprobe system with Ar ion laser ($\lambda=514.5$ nm) in backscattering geometry was used for polarized and temperature-dependent Raman scattering.

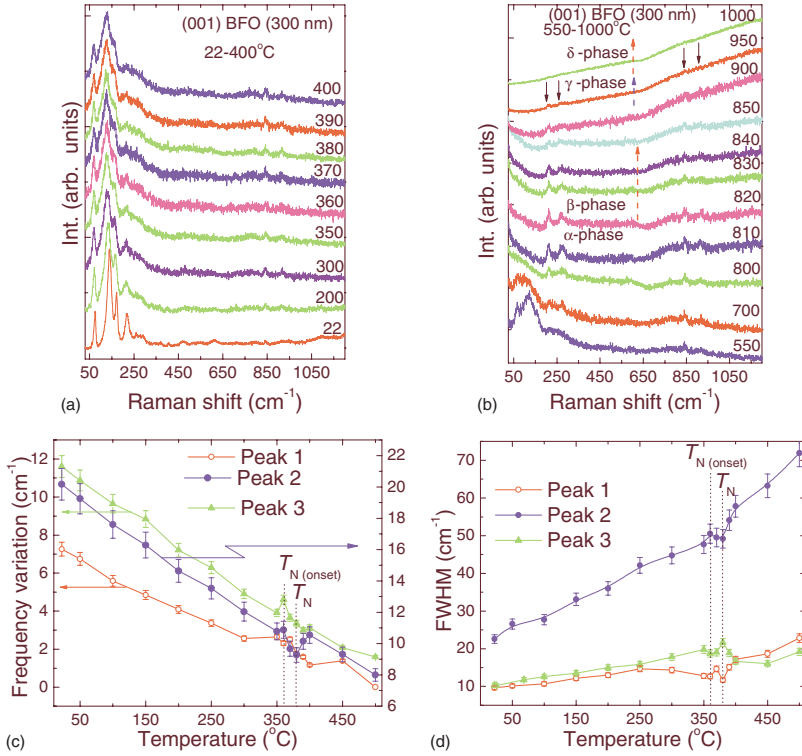


FIG. 1. (Color online) Temperature-dependent Raman spectra of (001)BFO film on SRO/STO from (a) 22–400 °C and (b) 550–1000 °C. The graphs in (b) were adapted from our earlier work (Ref. 12). The beginning of the *dashed arrows* pointing up in (b) shows the beginning of the new phase. The existence of phonons in γ phase in (b) are marked with the solid arrows pointing down. The α phase extends up to 820 °C; (c) and (d) temperature dependence (RT–500 °C) of phonon frequencies variation and FWHM for 72 (peak 1), 140 (peak 2), and 171 (peak 3) cm⁻¹, respectively.

Sample deposition and experimental details are given in.¹²

The x-ray diffraction (XRD) pattern [see Fig. 2(a)] of the BFO films taken using Cu K_{α} (1.5406 Å) radiation show c -axis (pseudocubic $\langle 001 \rangle$ direction perpendicular to the substrate) orientation with a high degree of crystallinity. The c -axis length was found to be 3.95 Å, which implies epitaxial strain is quite relaxed. This agrees with the reported values ($c=3.997$ Å).¹⁹

The comparison of the unpolarized (perpendicular to the $\langle 001 \rangle$ of the substrate) Raman spectrum of BFO thin film with STO and SRO/STO spectra (cf. Fig. 2a in Ref. 12) precludes any Raman contribution from the substrate and bottom electrode; to the contrary, we observed a dip, rather than a peak, at the STO strongest peak position. As is evident from the intensity comparison, all of these peaks are due to the BFO normal modes of vibrations and none of them arose from the substrate. We verified our results using target materials, single crystals, and also by growing (001)BFO films on different substrates.

III. RESULTS AND DISCUSSION

A. Phonons in the γ phase

Figure 1 shows the temperature-dependent Raman spectra of (001)BFO film (300-nm thick) on SrTiO₃ substrates with SrRuO₃ buffer layer (25-nm thick). As can be seen from Fig. 1(b), four phonon features marked with arrows persist into the γ phase from 930–950 °C. Therefore this confirms an existence of noncubic γ phase. No first-order Raman scattering from phonons is allowed for cubic $Pm\bar{3}m$ (because each ion is at an inversion center, all phonons are odd parity). This is in agreement with the observation of an orthorhombic symmetry for the γ phase by Arnold *et al.*¹⁸ Although the

Raman lines are broad and weak at these temperatures, they exhibit no significant frequency shift at the β - γ transition at 930 °C; nor are there additional lines above or below 930 °C. Therefore it is very likely that the structure is $Pbnm$ in both β and γ phases and that no primitive-to-body-centered phase change occurs. Note that Fig. 1 is for a thin film. Therefore we conclude that the films do not differ from single crystals and powders previously studied with regard to the γ phase.

There is renewed interest in this β - γ transition because of the earlier discovery of a metal-insulator transition at 931 °C where the orthorhombic-cubic transition takes place in bulk¹² and that the same transition may occur at 47 GPa at RT. Earlier Mössbauer studies established that at this pressure the magnetization also disappears.²⁰ Although Gavriliuk *et al.*²⁰ concluded that this is a rhombohedral-rhombohedral symmetry-preserving Mott transition, that seems quite unlikely, because Haumont *et al.*²¹ have found several phase transitions at lower pressure. Thus the symmetry of BiFeO₃ is not rhombohedral on either side of the high-pressure metal-insulator transition. Whether the transition is a Mott transition or a band transition is unproven. Various theoretical models disagree: Gonzalez-Vasquez *et al.*²² get an *ab initio* Mott transition; Clark and Robertson²³ got a band transition to a semimetal from a screened exchange model.

Figures 1(a) and 1(b) show the temperature variation (from RT up to 1000 °C) of unpolarized Raman spectra of a BFO(001) thin film. A closer observation near the phase transitions reveals two noticeable changes in the signature of the Raman spectra: the disappearance of several stronger modes at ~ 820 °C and the complete disappearance of all the modes around 1000 °C. This temperature behavior implies that BFO maintains its room temperature structure up to ~ 820 °C, indicating the structural (ferroelectric) phase tran-

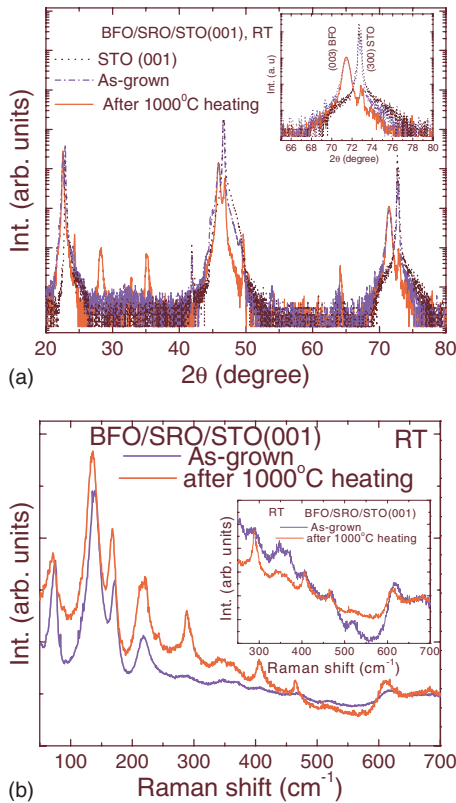


FIG. 2. (Color online) Room-temperature XRD patterns taken using (a) $\text{Cu } K_{\alpha}$ (1.5406 \AA) radiation and (b) Raman spectra of (001)BFO film on SRO/STO before and after thermal cycle up to $1000 \text{ }^{\circ}\text{C}$. XRD pattern of STO is given for comparison.

sition, in agreement with the earlier investigations on BFO bulk single crystal and polycrystalline samples.²⁴ Note that thin films of BFO show first-order phase transitions as in bulk whereas STO and PbTiO_3 (PTO) are known to be first order in bulk but second order in thin films.^{25,26}

The presence of the four peaks (~ 213 , 272 , 820 , and 918 cm^{-1}) above $820 \text{ }^{\circ}\text{C}$ up to $\sim 950 \text{ }^{\circ}\text{C}$ [Fig. 1(b)] shows that the intermediate beta phase is *not* cubic ($Pm\bar{3}m$) as reported by Haumont *et al.*²⁴ In fact, the phase diagram of BFO,²⁷ and its more recent revised versions,¹² show that BFO possesses a noncubic β phase between 820 and $933 \text{ }^{\circ}\text{C}$ before it goes to the γ phase, and the β phase was recently shown to be orthorhombic by using high temperature x-ray diffraction and domain structures¹² and neutron diffraction.¹⁸ The complete disappearance of peaks at above $950 \text{ }^{\circ}\text{C}$ —*not* at $930 \text{ }^{\circ}\text{C}$ —indicates that the γ high-temperature phase also cannot be cubic ($Pm\bar{3}m$), for which any first-order Raman scattering is forbidden.

Figure 2(a) shows the room-temperature XRD patterns of an as-grown film and film after it underwent $1000 \text{ }^{\circ}\text{C}$ thermal cycle. As can be seen, the as-grown film is highly epitaxial showing only (001) peaks and became polycrystalline after thermal cycling. In principle, it is possible that the specimen would melt at high temperatures and then recrystallize in the specimen holder (bottom of the Pt crucible). However, we monitored the sample surface continuously with an optical microscope and no thermal decomposition was observed up to $1000 \text{ }^{\circ}\text{C}$.

The Raman spectra [Fig. 2(b)] before and after heating show *exactly* same number of phonon modes, indicating either no decomposition up to $1000 \text{ }^{\circ}\text{C}$ or complete recrystallization, contrary to earlier studies,¹⁴ which could be due to the reduced surface/volume ratio, minimal surface imperfections and defects, and increased stabilization from the substrate. Note that the possibilities of subtle structural changes (small changes on angles and/or in-plane lattice parameters) cannot be completely ruled out. However, the Raman frequencies before and after thermal cycling remain unchanged makes this unlikely. This fact favors films over bulk or powder samples for very high temperature studies in the future. Reaching the tetragonal and cubic phases extrapolated from the powder study of Arnold *et al.*²⁸ does not seem impossible with thin films.

B. Phonon anomalies near T_N

There are discrepancies in the literature regarding both the crystal structure of (001)BFO thin films, e.g., with several reports claiming tetragonal,^{3,29} rhombohedral,^{30,31} and monoclinic^{19,32} structure, and its phonons. Of particular interest regarding phonon-magnon coupling in BFO was the report²⁴ of a very large (40 cm^{-1}) change in the frequency of one long wavelength phonon branch near T_N . We emphasize in the present work that we see no such phenomenon [Fig. 1(a)]. Instead we see in Figs. 1(c) and 1(d) very small changes in frequency (1 or 2 cm^{-1}) and linewidth of several polar modes, and we model them according to the nonmean-field theory of Nugroho *et al.*³³

In general, there are three kinds of phonon anomalies observed near the phase-transition temperatures: a sigmoidal S -shaped change in frequency (such as that reported by Haumont *et al.*²⁴ but not found in our work); a step discontinuity; or a small “bump” (increase) that returns to the background level a few degrees above or below the transition temperature.

In order to study the evolution of Raman signature around the AFM-paramagnetic (PM) phase transition, we followed very closely the temperature dependence of few intense phonon modes, i.e., 72 (Peak 1, we considered it as single peak for the simplicity), 140 (Peak 2), and 171 (Peak 3) cm^{-1} from RT up to $500 \text{ }^{\circ}\text{C}$ [Fig. 1(a)]. In general, the change in phonon frequency band and width with temperature can be caused by several factors, such as anharmonic scattering, spin-phonon coupling, lattice expansion and/or contraction due to anharmonicity and/or magnetostriction effects, and phonon renormalization resulting from electron-phonon coupling.³⁴ The latter one is not applicable here as BFO is a highly resistive material and the carrier concentration is low. The change in ionic binding energies with temperature also affects the change in phonon bandwidth in ionic compounds. However, this is not applicable here as BFO is insulating. Figures 1(c) and 1(d) reveal the fluctuation of phonon frequency and full width at half maxima (FWHM) around $370 \text{ }^{\circ}\text{C}$ (onset could be $\sim 360 \text{ }^{\circ}\text{C}$), which happens to be the T_N of BFO. Near T_N we see small (1 or 2 cm^{-1}) changes in both peak frequency and linewidth for three phonon modes at 72 , 140 , and 171 cm^{-1} . These satisfy the nonmean-field

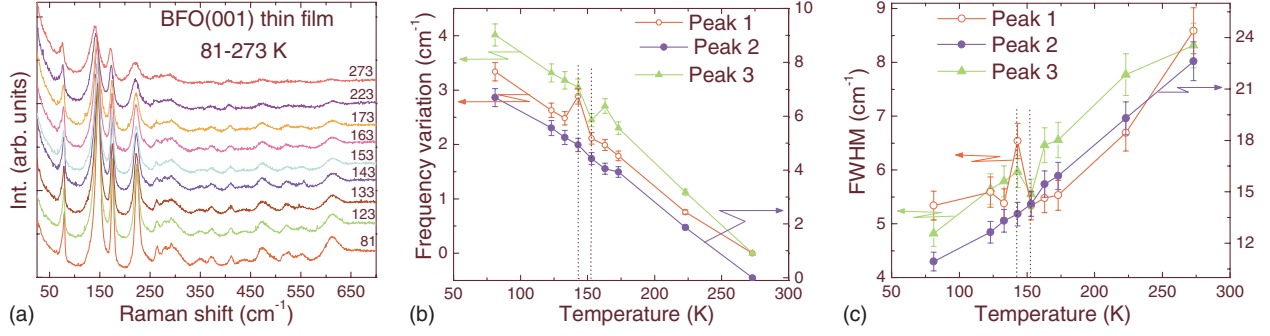


FIG. 3. (Color online) (a) Temperature-dependent Raman spectra of (001)BFO film on SRO/STO from 81 K-RT; (b) and (c) temperature dependence of phonon frequencies variation and FWHM for 72 (peak 1), 140 (peak 2), and 171 (peak 3) cm⁻¹ down to 81 K from RT, respectively.

predictions of Nugroho *et al.*³³ This behavior could be the manifestation of phonon-magnon interaction that vanishes above T_N , 370 °C. This weak interaction can be explained with the fact that the magnetic phase transition is not accompanied by a structural phase change. The observation of a rather weak phonon-magnon interaction is also consistent with the theoretical prediction of weak magnetization and ME coupling in BFO thin film by Ederer and Spaldin.³⁵

C. Phonon anomalies near 140–150 K

In order to study the cryogenic behavior of BFO thin films, we carried out scattering measurements [Fig. 3(a)] down to 81 K; no significant change in Raman spectra has been observed, indicating the RT structure remained unchanged down to 81 K. However, a close observation shows phonon anomalies around 150 K [Figs. 3(b) and 3(c)]. This agrees with the observation of change in magnetic order at 150 K by Pradhan *et al.*,³⁶ but the nature of this phase transition remains moot.

Figures 3(b) and 3(c) show small anomalies in the frequency and linewidth of two phonon branches at 140 and 171 cm⁻¹ near 140 K, a temperature at which anomalies have previously been reported. Although the changes are small and the data sparse, they are highly reproducible. We are aware of similar observations on single crystals by Dkhi³⁷ and we thank him for preprints of his work. The present data merely show that the same effects are present in thin films.

The nature of the phase transition at 140 K remains unknown. There are anomalies in magnetization and magnon scattering cross sections^{38–42} and linewidth,^{43,44} in mechanical loss tangent^{38,45} and 140 K is the end point in Almeida-Thouless data plots.^{43,44} However, the earlier suggestion by our group⁴⁶ that 140 K is a spin-reorientation transition temperature is not confirmed by very recent neutron-scattering studies⁴⁷ and spin-glass effects⁴⁸ have also been suggested but are unproven.

D. Weak phonon-magnon coupling

In our Raman spectra [Figs. 1(c) and 1(d)] we observed small (1 or 2 cm⁻¹) increases or decreases in phonon frequencies very near T_N . Note that this is observed for several different phonon symmetries. The symmetry independence

of the phonon-magnon coupling implies an interaction of form P^2M^2 (where P and M are the polarization and magnetization, respectively) in the free energy, as first suggested for magnetoelectrics by Smolenskii and Chupis.¹⁰ In general, the coupling of phonons and magnons can occur through several different microscopic physical models: the Torrance-Slonczewski model⁴⁹ involves modulation of the crystal field at the spin site by the optical phonon and is significant for ions with unquenched orbital angular momenta, such as Co⁺² or Fe⁺²; the model of Buyers *et al.*⁵⁰ is an angular momentum coupling of spins in octahedra where the optical phonon eigenvector is rotationlike as viewed from the magnetic ion. However, such models do not give frequency anomalies near T_N like those we observed in BiFeO₃. A rather detailed model of magnetocapacitance was given by Fox *et al.*⁵¹ for BaMnF₄ near T_N , and related models by Scott⁵² and by Glass *et al.*⁵³ for the BaMF₄ family near the two-dimensional spin-ordering temperature (T) (typically $\sim 3T_N$ in that family). The free energy of Fox *et al.*⁵¹ can be defined as

$$G = f(L^2, L_z^2) + BM^2 + (b_0 + b_1p + b_2p^2)M_xL_z + \dots, \quad (1)$$

where P is along y , the polar axis and z is the sublattice magnetization direction; L is $(1/2)g\mu S^{1/2}(S+1)^{1/2}[\Sigma(S_j \text{ up} - S_j \text{ down})]$ and M is the weak magnetization $M = g\mu S^{1/2}(S+1)^{1/2}[\Sigma(S_j \text{ up} + S_j \text{ down})]$. Note that p is not the total polarization P but only the part induced by the magnetoelectric coupling: $P = P_r + p$ and it was carried out to second order in polarization P , sublattice magnetization M , and weak ferromagnetization L , with the result that the magnetocapacitance varies with temperature as $(b_0 - b_1b_2)L_z(T)$, where b_0 , b_1 , and b_2 are, respectively, the coefficients of magnetoelectric free-energy terms independent of, linear in, and quadratic in polarization P . The authors noted that the mean-field theory, although generally not satisfactory for magnetic transitions, works well for weakly canted ferromagnets because the expansion parameter L is small at all temperatures. Note that the sign of the magnetocapacitance term can be positive or negative depending upon the magnitude of $(b_0 - b_1b_2)$. Because they used mean field theory, their work neglected the small term near T_N due to fluctuations considered below.

Although the second-order theory of Fox *et al.*⁵¹ was satisfactory for describing all the data in BaMnF₄ near T_N , it is

not sufficient for phonon behavior in BiFeO₃. In this case it is necessary to go to fourth order in L . The reasons are explained by Nugroho *et al.*³³ in their work on YbMnO₃. In this case the key term in the free energy is of the form gP^2L^2 , which for weak coupling gives an explicit interaction of electric field to L that results in a magnetocapacitance of

$$(g^2P^2/kT) \int [\langle L^2(x)L^2(0) \rangle - \langle L^2 \rangle^2] dx. \quad (2)$$

Although this fourth-order term is higher order than the terms in $g\langle L^2 \rangle$ considered by Fox *et al.*,⁵¹ it is singular at T_N , because it is proportional to the cube of the correlation length (η) that diverges at T_N .

The result is that the phonons in Raman effect in BiFeO₃ of any symmetry will be expected to have small anomalies in their frequencies at T_N . These small dips or jumps will be proportional to temperature $t^{(\alpha-1)}$,^{33,54} where t is reduced temperature, $t=[T_N-T]/T_N$ and α is the critical exponent describing divergence of the specific heat.⁵⁵ Since the α is typically small, the phonon frequencies should vary approximately as $T_N/[T_N-T]$ near T_N and, in principle, could be used to evaluate critical exponent α . However in the present work the data are too imprecise for this chore and even higher resolution would be insufficient due to phonon damping. The bump in phonon frequencies and linewidth are qualitatively predicted from the nonmean-field theory of Nugroho *et al.*³³ However, their model does not predict magnitudes for the height (increase in frequency) or width (how near the transition the increase occurs) of the bump. No anomaly at all is predicted by the mean-field theory of Fox *et al.*,⁵¹ which does not consider terms in the free energy introduced by Nugroho *et al.*³³ A similar behavior has been observed at 150 K [Figs. 3(b) and 3(c)] could be due to the change in magnetic ordering.³⁶ As matter of coincidence the bottom electrode SRO has a ferromagnetic phase transition at 150 K. Note that none of these peaks is related to SRO and a modulated effect is highly unlikely but not impossible.

In summary, our Raman frequencies near T_N and 150 K show small peaks or dips for all phonon modes that are qualitatively similar to those predicted by Nugroho *et al.*,³³ implying a general interaction of form P^2L^2 , and the need for a fluctuation term neglected in the mean-field, weak ferromagnetism model of Fox *et al.*⁵¹

IV. CONCLUSION

In conclusion, high-quality epitaxial (001)BFO films have been grown on (100)STO substrates using PLD. The XRD studies showed that films are c -axis oriented with high degree of crystallinity. The RT-polarized Raman scattering of (001)BFO films showed pseudo-orthorhombic monoclinic crystal structure contrary to the rhombohedral and tetragonal symmetries reported earlier. We observed the ferroelectric phase transition at around 820 °C and no softening of Raman modes was observed at low frequencies, as in BFO single crystals. The AFM-PM phase transition at around 370 °C caused some small changes in the phonon frequencies, linewidth, and/or intensities of several low-frequency modes, indicating ME coupling in the material. A noncubic γ -BiFeO₃ phase was observed between 931–950 °C in the BFO thin films, in agreement with the accepted BiFeO₃ phase diagram. The spectra also revealed an evidence of a cubic δ phase around 1000 °C in thin films that is not stable in powder and bulk.

ACKNOWLEDGMENTS

The authors are grateful to Hans Schmid, University of Geneva for supplying BFO single crystal for the comparative study with the thin film and G. Catalan, University of Cambridge for his useful comments and suggestions. We thank Brahim Dkhil for sharing his Raman data on phonon anomalies in BFO single crystals near 140 K prior to their publication. The authors would like to acknowledge financial support from DOE under Grant No. DE-FG02-08ER46526. R.P. thanks Institute of Functional Nanomaterial (IFN), UPR for financial support.

*r.palai@uprrp.edu

¹H. Schmid, *Ferroelectrics* **162**, 317 (1994).

²M. Fiebig, T. Lottermoser, D. Fröhlich, A. V. Goltsev, and R. V. Pisarev, *Nature (London)* **419**, 818 (2002).

³J. Wang, J. B. Neaton, H. Zheng, V. Nagarajan, S. B. Ogale, B. Liu, D. Viehland, V. Vaithyanathan, D. G. Schlom, U. V. Waghmare, N. A. Spaldin, K. M. Rabe, M. Wuttig, and R. Ramesh, *Science* **299**, 1719 (2003).

⁴Y. Tokura, *Science* **312**, 1481 (2006).

⁵J. F. Scott, *Nature Mater.* **6**, 256 (2007).

⁶T. Zhao, A. Scholl, F. Zavaliche, K. Lee, M. Barry, A. Doran, M. P. Cruz, Y. H. Chu, C. Ederer, N. A. Spaldin, R. R. Das, D. M. Kim, S. H. Baek, C. B. Eom, and R. Ramesh, *Nature Mater.* **5**, 823 (2006).

⁷Y. H. Chu, M. P. Cruz, C. H. Yang, L. W. Martin, P.-L. Yang, J.-X. Zhang, K. Lee, P. Yu, L.-Q. Chen, and R. Ramesh, *Adv.*

Mater. (Weinheim, Ger.) **19**, 2662 (2007).

⁸N. A. Hill, *J. Phys. Chem. B* **104**, 6694 (2000).

⁹I. Sosnowska, T. Peterlin-Neumaier, and E. Steichele, *J. Phys. C* **15**, 4835 (1982).

¹⁰G. A. Smolenskii and I. Chupis, *Sov. Phys. Usp.* **25**, 475 (1982).

¹¹C. Tabares-Munoz, J. P. Rivera, and H. Schmid, *Ferroelectrics* **55**, 235 (1984).

¹²R. Palai, R. S. Katiyar, H. S. Schmid, P. Tissot, S. J. Clark, J. Robertson, S. A. T. Redfern, G. Catalan, and J. F. Scott, *Phys. Rev. B* **77**, 014110 (2008).

¹³F. Kubel and H. Schmid, *Acta Crystallogr., Sect. B: Struct. Sci.* **46**, 698 (1990).

¹⁴J. D. Bucci, B. K. Robertson, and W. J. James, *J. Appl. Crystallogr.* **5**, 187 (1972).

¹⁵M. Polomska, W. Kaczmarek, and Z. Pajak, *Phys. Status Solidi A* **23**, 567 (1974).

- ¹⁶V. V. Shvartsman, W. Kleemann, R. Haumont, and J. Krisel, *Appl. Phys. Lett.* **90**, 172115 (2007).
- ¹⁷D. Lebeugle, D. Colson, A. Forget, M. Viret, P. Bonville, J. F. Marucco, and S. Fusil, *Phys. Rev. B* **76**, 024116 (2007).
- ¹⁸D. C. Arnold, K. S. Knight, F. D. Morrison, and P. Lightfoot, *Phys. Rev. Lett.* **102**, 027602 (2009).
- ¹⁹G. Xu, H. Hiraka, G. Shirane, J. Li, J. Wang, and D. Viehland, *Appl. Phys. Lett.* **86**, 182905 (2005).
- ²⁰A. G. Gavriliuk, V. V. Struzhkin, I. S. Lyubutin, M. Y. Hu, and H. K. Mao, *JETP Lett.* **82**, 224 (2005).
- ²¹R. Haumont, P. Bouvier, A. Pashkin, K. Rabia, S. Frank, B. Dkhil, W. A. Crichton, C. A. Kuntscher, and J. Kreisel, *Phys. Rev. B* **79**, 184110 (2009).
- ²²O. E. Gonzalez-Vazquez and J. Iniguez, *Phys. Rev. B* **79**, 064102 (2009).
- ²³S. J. Clark and J. Robertson, *Appl. Phys. Lett.* **90**, 132903 (2007).
- ²⁴R. Haumont, J. Kreisel, P. Bouvier, and F. Hippert, *Phys. Rev. B* **73**, 132101 (2006).
- ²⁵G. Catalan, A. Janssens, G. Rispens, S. Csiszar, O. Seeck, G. Rijnders, D. H. A. Blank, and B. Noheda, *Phys. Rev. Lett.* **96**, 127602 (2006).
- ²⁶F. He, B. O. Wells, and S. M. Shapiro, *Phys. Rev. Lett.* **94**, 176101 (2005).
- ²⁷E. I. Speranskaya, V. M. Skorikov, E. Y. Rode, and V. A. Terekhova, *Bull. Acad. Sci. USSR Div. Chem. Sci.* **14**, 873 (1965).
- ²⁸D. C. Arnold, P. Lightfoot, G. Catalan, J. F. Scott, and F. D. Morrison, *Phys. Rev. B* (to be published).
- ²⁹M. K. Singh, S. Ryu, and H. M. Jang, *Phys. Rev. B* **72**, 132101 (2005).
- ³⁰R. R. Das, D. M. Kim, S. H. Baek, C. B. Eom, F. Zavaliche, S. Y. Yang, R. Ramesh, Y. B. Chen, X. Q. Pan, X. Ke, M. S. Rzchowski, and S. K. Streiffer, *Appl. Phys. Lett.* **88**, 242904 (2006).
- ³¹X. Qi, J. Dho, R. Tomov, M. G. Blamire, and J. L. MacManus-Driscoll, *Appl. Phys. Lett.* **86**, 062903 (2005).
- ³²J. Li, J. Wang, M. Wuttig, R. Ramesh, N. Wang, B. Ruetter, A. P. Pyatakov, A. K. Zvezdin, and D. Viehland, *Appl. Phys. Lett.* **84**, 5261 (2004).
- ³³A. A. Nugroho, N. Bellido, U. Adem, G. Nenert, C. Simon, M. O. Tjia, M. Mostovoy, and T. T. M. Palstra, *Phys. Rev. B* **75**, 174435 (2007).
- ³⁴E. Granado, A. Garcia, J. A. Sanjurjo, C. Rettori, I. Torriani, F. Prado, R. Sanchez, A. Caneiro, and S. B. Oseroff, *Phys. Rev. B* **60**, 11879 (1999).
- ³⁵C. Ederer and N. A. Spaldin, *Phys. Rev. B* **71**, 060401(R) (2005).
- ³⁶A. K. Pradhan, K. Zhang, D. Hunter, J. B. Dadson, B. Loutts, P. Bhattacharya, R. S. Katiyar, J. Zhang, D. J. Sellmyer, U. N. Roy, Y. Cui, and A. Burger, *J. Appl. Phys.* **97**, 093903 (2005).
- ³⁷B. Dkhil (private communication).
- ³⁸G. Catalan and J. F. Scott, *Adv. Mater. (Weinheim, Ger.)* **21**, 2463 (2009).
- ³⁹M. K. Singh, R. S. Katiyar, W. Prelier, and J. F. Scott, *J. Phys.: Condens. Matter* **21**, 042202 (2009).
- ⁴⁰M. Cazayous, Y. Gallais, A. Sacuto, R. de Sousa, D. Lebeugle, and D. Colson, *Phys. Rev. Lett.* **101**, 037601 (2008).
- ⁴¹P. Rovillain, M. Cazayous, Y. Gallais, A. Sacuto, R. P. S. M. Lobo, D. Lebeugle, and D. Colson, *Phys. Rev. B* **79**, 180411(R) (2009).
- ⁴²B. Ramachandran and M. S. Ramachandra Rao, *Appl. Phys. Lett.* **95**, 142505 (2009).
- ⁴³J. F. Scott, M. K. Singh, and R. S. Katiyar, *J. Phys.: Condens. Matter* **20**, 425223 (2008).
- ⁴⁴J. F. Scott, M. K. Singh, and R. S. Katiyar, *J. Phys.: Condens. Matter* **20**, 322203 (2008).
- ⁴⁵S. A. T. Redfern, C. Wang, J. W. Hong, G. Catalan, and J. F. Scott, *J. Phys.: Condens. Matter* **20**, 452205 (2008).
- ⁴⁶M. K. Singh, R. S. Katiyar, and J. F. Scott, *J. Phys. Condens. Matter* **20**, 252203 (2008).
- ⁴⁷J. Herrero-Albillos and G. Catalan (unpublished).
- ⁴⁸M. K. Singh, W. Prellier, M. P. Singh, R. S. Katiyar, and J. F. Scott, *Phys. Rev. B* **77**, 144403 (2008).
- ⁴⁹J. B. Torrance and J. C. Slonczewski, *Phys. Rev. B* **5**, 4648 (1972); K. A. Hay and J. B. Torrance, *ibid.* **2**, 746 (1970).
- ⁵⁰T. M. Holden, W. J. L. Buyers, E. C. Svensson, R. A. Cowley, M. T. Hutchings, D. Hukin, and R. W. H. Stevenson, *J. Phys. C* **4**, 2127 (1971); W. J. L. Buyers, T. M. Holden, E. C. Svensson, R. A. Cowley, and M. T. Hutchings, *ibid.* **4**, 2139 (1971).
- ⁵¹D. L. Fox, D. R. Tilley, J. F. Scott, and H. J. Guggenheim, *Phys. Rev. B* **21**, 2926 (1980).
- ⁵²J. F. Scott, *Phys. Rev. B* **16**, 2329 (1977).
- ⁵³A. M. Glass, M. E. Lines, M. Eibschutz, F. S. L. Hsu, and H. J. Guggenheim, *Commun. Phys. (London)* **2**, 103 (1977).
- ⁵⁴M. Mostovoy (private communication).
- ⁵⁵A. Munoz, J. A. Alonso, M. J. Martinez-Lope, M. T. Casais, J. L. Martinez, and M. T. Fernandez-Diaz, *Phys. Rev. B* **62**, 9498 (2000).